Importance of bound-free correlation effects for vibrational excitation of molecules by electron impact: A sensitivity analysis

Michael A. Morrison* and Wayne K. Trail
Joint Institute for Laboratory Astrophysics, University of Colorado and National Institute of Standards and Technology, Boulder, Colorado 80309-0440
(Received 24 February 1993)

One of the most interesting, important, and problematic components of interaction potentials for electron-atom and -molecule scattering arises from many-body effects in the near-target region. Such "core-polarization" effects are of particular concern for vibrational-excitation calculations, where these short-range bound-free correlation and nonadiabatic velocity-dependent effects have remained resistant to rigorous treatment, being represented instead by approximations or model potentials. In order to provide guidance for assessing such potentials and insight into the nature of these many-electron effects, we have investigated the sensitivity to core polarization of total, momentum-transfer, rotational-excitation, and vibrational-excitation e-H_2 cross sections. The sensitivity analysis for the latter cross section also comments on a long-standing, severe discrepancy [most recently documented in S. J. Buckman *et al.*, Phys. Rev. Lett. **65**, 3253 (1990)] between cross sections determined in various crossed-beam experiments and by transport analysis of swarm data for this simplest electron–neutral-molecule system.

PACS number(s): 34.80.Gs

I. INTRODUCTION

The behavior of low-energy electrons in collisions with atoms and molecules is controlled by three kinds of interactions: electrostatic, exchange, and polarization [1–3]. Outside the region of localization of the target charge density, a region we shall refer to as the "core", the latter interaction can be understood as an induced effect arising from distortions of the molecular electronic wave function by the charged projectile [4]. Rigorously, this effect arises in quantum collision theory as virtual excitations of closed electronic states—including, in principle, those in the continuum [5]. In practice, however, the infinity of such states precludes treating polarization rigorously. So considerable theoretical effort has been expended over the past three decades trying to include it accurately but nonrigorously.

What makes this so difficult is not representing the deformation of the target density by a charge fixed some ways from the origin but rather the effects which come into play near and within the core. Well beyond the target, the velocity of the projectile is low enough that the bound molecular electrons respond as though it were "frozen;" that is, the projectile's motion can be treated adiabatically [6]. But as the projectile nears the target, it experiences an increasingly strong attractive (Coulomb) field, and its local kinetic energy may become so large that the response of the target becomes dependent on the projectile's velocity, in which case the polarization potential becomes dependent on the scattering energy [7]. Worse, where the projectile's wave function overlaps the core, the scattering electron loses its identity, the independent-particle model breaks down, and many-body effects predominate. The polarization potential at short range is therefore not only energy dependent but also nonlocal. To distinguish these different physical regions we shall refer to the short-range effects as "core polarization" and to the totality of these effects throughout configuration space as "correlation-polarization."

Widespread interest in many-body effects, persistent discrepancies among experimental results [8], and the acknowledged importance of polarization for low-energy electron scattering have all driven research during the past two decades on this component of the interaction—including the present study [9,10]. The most rigorous treatments of correlation and polarization effects involve either pseudostates [11] or, more commonly, an optical potential [12,13]. The latter retains a single-particle description of the collision by dumping all the many-body effects into a complex, nonlocal, energy-dependent effective potential. One can construct optical potentials in a variety of ways: e.g., using the self-energy of the one-particle Green's function [14] or via Feschbach projection of a configuration-interaction wave function [15]. In the latter category fall [16] implementations such as the R-matrix [17], the Schwinger-variational [18], and Kohn-variational methods [19]. Accurate calculation of a converged optical potential for electron-molecule systems often requires enormous basis sets and a major investment of computer time. Perhaps for this reason all such studies published to date have made the rigid-rotor approximation, fixing the internuclear geometry of the target at equilibrium. This approximation, obviously, precludes study of vibrational excitation, which depends critically on the variation of the interaction potential with internuclear separation, except in adiabatic treatments of the vibrational motion, which are valid only at energies above several eV [20,21].

If the vibrational dynamics must be explicitly coupled to the motion of the projectile, as in vibrational close-coupling calculations [22], it is infeasible to treat correlation and polarization effects via an optical potential.

Hence all such calculations to date have included these effects via model potentials [23–25]. The model-potential approach strives to treat the single-particle aspects of this phenomenon as accurately as possible while approximating short-range many-body core-polarization effects. Ideally, model correlation-polarization potentials should be free of parameters requiring adjustment to experimental cross section; it is in this sense that they are often described as *ab initio*.

One such model, which we have used in a series of investigations of e-H_2 and e-N_2 scattering [21–28], uses a short-range approximation [29] to improve on a purely adiabatic polarization potential; for reasons explained in detail elsewhere [24,30,31] we have named this model the "better-than-adiabatic dipole" (BTAD) potential. This local, energy-independent potential is based on an accurate variational treatment of (adiabatic) polarization outside the core [32] and an approximate treatment of velocity-dependent and bound-free correlation at smaller distances [29,33], which facilitates its extension to a variety of systems and scattering processes [28]. For low-energy *vibrationally elastic* scattering from H_2 and N_2 we have shown that the BTAD potential accurately represents the influence of correlation and polarization effects on total, rotational, and momentum-transfer cross sections—at least as judged by comparison to experimental data [21,28].

We have also used this potential in calculations of vibrational-excitation cross sections [23,27], for which there are no more rigorous theoretical results and existing experimental data is contradictory [8,27].

The experimental situation is particularly acute. In spite of extensive collaborative efforts for over a decade by theorists [23,27,34] and two groups of experimentalists [27,34,35] to determine agreed-upon cross sections for this scattering process, there remains a serious, inexplicable discrepancy in the $0\rightarrow 1$ vibrational cross section $\sigma^{(v)}_{0\rightarrow 1}$ at energies below about 3.0 eV, as seen in Fig. 1 [34]. For excitation of the $v=1$ vibrational manifold at 1.5 eV, for example, the results from swarm and beam experiments differ by 77%, well outside the claimed error bars for both [27,35].

This long-standing disagreement first appeared in comparisons of cross sections derived via transport analysis of data taken in swarm experiments [36–40] with integrated normalized angular distributions measured in crossed-beam experiments [41–43]. Its severity and intractability motivated a recent state-of-the-art crossed-beam measurement of elastic and vibrational cross sections—which produced results in agreement with the earlier beam data [44,45]. Theoretical cross sections based on the BTAD potential, agree quite well with the most recent beam data up to about 2 eV, beyond which the situation is less clear [27,35].

Exhaustive efforts by all concerned have failed to resolve this discrepancy. Recent analyses of swarm data for mixtures of H_2 and various rare gases yield cross sections that agree with a reanalysis of earlier transport coefficients for pure H_2 [46]. A more recent study shows the latest beam and theoretical vibrational cross sections at energies as high as 3 eV to be incompatible with these transport coefficients [35].

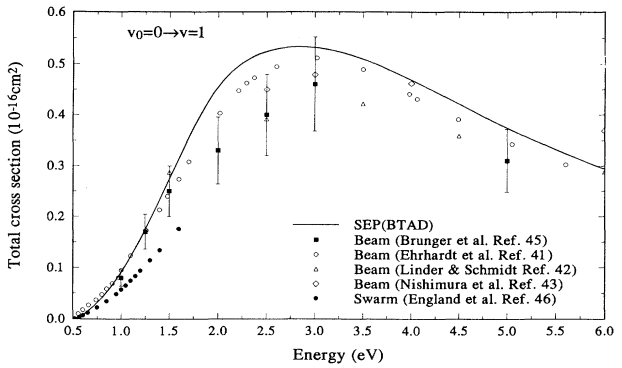

FIG. 1. Integrated $0\rightarrow 1$ vibrational excitation e-H_2 cross sections: theoretical results from BTAD (SEP) calculations of Refs. [57] (curve) and experimental data from beam experiments by Ehrhardt *et al.* (Ref. [41]) (open circles), Linder and Schmidt (Ref. [42]) (triangles), Nishimura, Danjo, and Sugahara (Ref. [43]) (diamonds), and Brunger, Buckman, and Newman (Ref. [44]) (boxes with error bars), and from transport analysis of swarm data by England, Elford, and Crompton (Ref. [46]) (closed circles).

This highly unsatisfactory situation provided a second motivation for the present study. For very-low-energy collisions, swarm experiments remain the sole experimental source of accurate inelastic and momentum-transfer cross sections for atomic as well as molecular targets [47]. Indeed, transport analysis has provided valuable data for electron scattering from such molecules as H_2 [38,39,48,49], D_2 [49], N_2 [50], O_2 [51], CO_2 [51–53], CO [51,54], H_2O [55], and CH_4 [56].

The paramount importance of swarm analyses at low energies and our conviction that it should be possible, at least for this simplest system, for swarm analysis, beam experiments, and theory to produce uniform cross sections have driven successive enhancements to our theoretical formulation [34,27,57]. These improvements, however, have increased the level of rigor without significantly changing the cross sections. The present formulation (summarized in Sec. II B), based on full inclusion of the vibrational dynamics and an exact treatment of nonlocal exchange effects, contains only one significant approximation: the representation of short-range core-polarization effects in the BTAD potential (see Sec. II B).

In the hopes of shedding light on this discrepancy and, more generally, on the physics of short-range bound-free correlation in electron-molecule scattering, we have undertaken the present study of the importance of core-polarization effects for various e-H_2 cross sections. Our goal is a quantitative understanding of the sensitivity of relevant low-energy (electronically elastic) cross sections to these effects. By identifying the most sensitive cross sections (and energy ranges thereof), we also hope to provide a context for assessing the accuracy of various model and basis-set potentials and for deciding whether more rigorous (and demanding) treatments, such as one based on an optical potential, are warranted. In the next sec-

tion we summarize the relevant scattering theory and the physics of the BTAD potential. In Sec. III we examine various polarization potentials, define a quantitative measure of the importance of core polarization, and present sensitivity analyses for total, momentum-transfer, rotational, and vibrational cross sections. Finally in Sec. IV we address the implications of this work for experimental and theoretical concerns noted above.

II. THEORY

Elsewhere we have described our theoretical formulation of the low-energy electron-molecule collision problem [21], the numerical methods we use to solve the Schrödinger equation to obtain the scattering matrix [57], and our treatment of various components of the interaction potential [26]. In the present section, therefore, we shall only summarize the theoretical context of this study, noting aspects that are germane to the analysis in Sec. III.

A. The scattering equations

We formulate the scattering problem in a body-fixed reference frame (with the z axis coincident with the internuclear axis $\hat{\mathbf{R}}$) and make the fixed-nuclear-orientation approximation, according to which we neglect the rotational Hamiltonian during calculation of the scattering matrix [58–60]. This amounts to treating the rotational motion of the target adiabatically [61], an approximation which is quite accurate at energies of interest here [26], above the first vibrational threshold 0.52 eV. The fixed nuclear orientation approximation does not, however, preclude the study of rotational excitation; if desired we can reintroduce the rotational dynamics "after the fact" via a rotational frame transformation of the scattering matrix [59].

Within this conceptual scheme we project out of the full time-independent electron-molecule wave function the ground electronic state of the target (in the Born-Oppenheimer approximation) [3], thereby obtaining a "reduced" wave function that depends only on the projectile coordinate $\mathbf{r}_e$ and the internuclear separation R.

To convert the resulting reduced Schrödinger equation into a set of coupled radial differential equations we expand the wave function in a basis of products of vibrational wave functions of the (undistorted) target, $\phi_v^{(v)}(R)$, and spherical harmonics [21,62]. We calculate the vibrational functions, the eigenfunctions of the (Born-Oppenheimer) nuclear Hamiltonian, by numerically solving the nuclear Schrödinger equation for the ground $X\,^1\Sigma_g^+$ electronic state in the near-Hartree-Fock limit. The spherical harmonics $Y_l^\Lambda(\theta_e,\varphi_e)$ are the angular functions appropriate to scattering from a linear molecule in the body frame; they are labeled by l, the quantum number for the orbital angular momentum of the projectile, and Λ, for its projection along the internuclear axis. These basis functions identify scattering channels with quantum numbers $(v,l;\Lambda)$.

Substitution of this expansion into the Schrödinger equation leads to an infinite set of coupled integrodifferential equations for the components of the radial scattering function, $u^\Lambda_{vl,v_0l_0}(r)$ (the coefficients in the aforementioned eigenfunction expansion), viz.,

$$\left[\frac{d^2}{dr^2}-\frac{l(l+1)}{r^2}+k_v^2\right]u^\Lambda_{vl,v_0l_0}(r)=2\sum_{v',l'}\left[V^\Lambda_{vl,v'l'}(r)+\hat{V}^\Lambda_{vl,v'l'}(r)\right]u^\Lambda_{v'l',v_0l_0}(r)\ , \tag{1}$$

where the channel energy $\frac{1}{2}k_v^2$ (in hartrees) is related to the total system energy E and the vibrational energy of the vth target state ε_v by energy conservation,

$$\tfrac{1}{2}k_v^2=E-\varepsilon_v\ . \tag{2}$$

In practice, of course, we must truncate this set of equations at some number of channels chosen to ensure convergence to a specified criterion of whatever scattering quantities are of interest: this is the close-coupling approximation [22,63].

Two coupling matrix elements appear in Eqs. (1) because we have identified two kinds of terms in the interaction potential: *local* terms, which appear in $V^\Lambda_{vl,v'l'}(r)$, and *nonlocal* terms in $\hat{V}^\Lambda_{vl,v'l'}(r)$. Here the local terms are the static potential [64,65] (the average of the two-particle bound-free Coulomb interactions over the ground electronic state) and the BTAD potential. These matrix elements are usefully expressed in terms of the Legendre projections $v_\lambda(r;R)$ of the local potentials, defined by

$$V_{\rm int}(\mathbf{r}_e;R)=\sum_{\lambda=0}^{\infty}{}'\,v_\lambda(r_e;R)P_\lambda(\cos\theta_e)\ , \tag{3}$$

where the prime indicates that the homonuclear symmetry of the molecule restricts the sum to even values of λ. In terms of these projections, the local matrix elements are [3,21]

$$V^\Lambda_{vl,v'l'}(r_e)=\sum_{\lambda=0}^{\infty}{}'\,g_\lambda(ll';\Lambda)\langle\phi_v^{(v)}|v_\lambda(r_e,R)|\phi_{v'}^{(v)}\rangle\ , \tag{4}$$

where the coupling coefficient is

$$g_\lambda(ll';\Lambda)=\left[\frac{2l'+1}{2l+1}\right]^{1/2}C(l'\lambda l;\Lambda 0)C(l'\lambda l;00)\ . \tag{5}$$

The nonlocal potential in the coupling matrix elements $\hat{V}^\Lambda_{vl,v'l'}(r)$ is simply the exchange potential, which appears in the reduce Schrödinger equation and hence in the coupled equations (1) because the full electron-molecule wave

function must be antisymmetric under pairwise particle interchange [66].

The present calculations incorporate an essentially exact treatment of exchange, the accuracy of which is limited only by the numerical precision of the solution of Eqs. (1). To solve these equations, we recast them using the linear-algebraic algorithm originally introduced to electron-molecule scattering by Schneider and Collins [67]. Its implementation begins with conversion of the integrodifferential equations (1) into coupled integral equations which incorporate the appropriate scattering boundary conditions [68,69]. Subsequent introduction of a quadrature into the integrals in these equations and discretization of the functions $u^{\Lambda}_{vl,v_0l_0}(r)$ renders the integral equations in matrix form. We solve the resulting set of coupled linear algebraic equations using standard linear-systems routines [70]. A significant virtue of this approach is that nonlocal operators such as $\hat{V}^{\Lambda}_{vl,v'l'}$ do not increase the dimensionality of these equations, making it ideal for problems involving such nonlocal potentials.

Solution of these equations yields the reactance matrix K defined by the boundary conditions

$$u^{\Lambda}_{vl,v_0l_0}(r) \underset{r\to\infty}{\sim} \hat{j}_{l_0}(k_{v_0}r)\delta_{ll_0}\delta_{vv_0} + K^{\Lambda}_{vl,v_0l_0}\hat{n}_l(k_v r) , \quad (6)$$

where $\hat{j}_{l_0}(k_{v_0}r)$ and $\hat{n}_l(k_v r)$ are Ricatti-Bessel-Neumann functions, respectively [12]. From this matrix we calculate the body-frame vibrational close-coupling (BFVCC) transition matrix [3,62]

$$\mathsf{T} = \frac{-2\mathsf{K}^2 + 2i\mathsf{K}}{1+\mathsf{K}^2} \quad (7)$$

and hence total, momentum-transfer, and vibrational-excitation cross sections.

These cross sections are suitable for comparison to results from experiments which do not resolve the *rotational* states of the target [44,71]. If we seek *pure rotational* ($v_0j_0 \to v_0j$) or *rovibrational* ($v_0j_0 \to v_j$) cross sections, we can use a rotational-frame transformation [3,59] to convert the BFVCC T matrix into one defined in the (space-fixed) laboratory frame, with the z axis chosen along the incident wave vector of the projectile, in a representation which couples the orbital angular momentum of the projectile to the rotational angular momentum of the target; this is the K matrix of conventional laboratory-frame close-coupling theory [63].

This rotational-frame transformation is equivalent to making the adiabatic-nuclear-rotation approximation [61]. At energies below a few tenths of an eV this approximation breaks down because it violates energy conservation [26]. (Although such energies are below the first vibrational threshold 0.52 eV, they are of interest in the present study for comparison to swarm-derived rotational cross sections.) We can improve significantly the accuracy of adiabatically determined rotational cross sections at these energies via a scaling procedure which ensures that elements of the T matrix which contribute to rotational excitation obey the correct threshold laws [72].

B. The polarization potential

As noted in Sec. I, the BTAD potential begins with a polarization potential that is adiabatic in that it neglects the *velocity* of the projectile [28,31]. This treatment is quite appropriate outside the core: beyond the region of strong electron-nuclear attraction, the projectile presents to the target a (negative) point charge at position $\mathbf{r}_e$ [73]. Indeed, such a picture is often used in calculations of atomic and molecular polarizabilities [74]. Under the influence of the electric field established by this charge, the molecular electrons (with collective spatial coordinates $\mathbf{r}_m$) relax into a state represented by the "polarized-core" wave function $\psi_0^p(\mathbf{r}_m;\mathbf{r}_e,R)$. Depending on the proximity of the projectile to the target, this wave function may differ considerably from the "frozen-core" ground-state Born-Oppenheimer electronic function $\psi_0(\mathbf{r}_m;\mathbf{r}_e,R)$. Consequently the energy of the system consisting of a fixed electron and the polarized target, $E_0^p(\mathbf{r},R)$, is lower than that of the projectile and the frozen (unpolarized) target, $E_0(\mathbf{r}_e,R)$. This energy difference is the adiabatic polarization potential,

$$V^A(\mathbf{r}_e;R) = E_0^p(\mathbf{r}_e,R) - E_0(\mathbf{r}_e,R) . \quad (8a)$$

Within the adiabatic picture we can calculate an accurate polarization potential using linear variational theory [30,75]. To this end we write this potential as the difference of two energy functionals,

$$V^A(\mathbf{r}_e;R) = \langle \psi_0^p(\mathbf{r}_m;\mathbf{r}_e,R)|\hat{\mathcal{H}}^A|\psi_0^p(\mathbf{r}_m;\mathbf{r}_e,R)\rangle - \langle \psi_0(\mathbf{r}_m;\mathbf{r}_e,R)|\hat{\mathcal{H}}^A|\psi_0(\mathbf{r}_m;\mathbf{r}_e,R)\rangle . \quad (8b)$$

The adiabatic Hamiltonian in these functionals is the sum of the (Born-Oppenheimer) electronic Hamiltonian of the molecule and the Coulomb potential for the interaction of the projectile (fixed at $\mathbf{r}_e$) with the constituents of the target,

$$\hat{\mathcal{H}}^A = \hat{\mathcal{H}}_m^{(e)}(\mathbf{r}_m;R) + V_{\rm em}(\mathbf{r}_m;\mathbf{r}_e,R) . \quad (9)$$

To evaluate Eq. (8b) we expand the polarized- and frozen-core wave functions in a basis chosen to span the relevant region of configuration space (from the origin to well outside the core) and to reproduce the measured values of the polarizability tensor of the target. The present calculations, for example, are based on optimized variational calculations at 11 values of R (from 0.5 to $2.60a_0$) using a basis of compact and diffuse Gaussian-type orbitals [23,24].

One way to corroborate the resulting potential is by examining its behavior at large r_e, where it must reduce to the asymptotic form (in atomic units)

$$V^A(\mathbf{r}_e;R) \underset{r_e\to\infty}{\sim} -\frac{\alpha_0(R)}{2r_e^4} - \frac{\alpha_2(R)}{2r_e^4}P_2(\cos\theta_e) , \quad (10)$$

with θ_e the scattering angle in the body frame. At each R, therefore, we extract the values of $\alpha_\lambda(R)$ from the Legendre projections [see Eq. (3)] of $V^A(\mathbf{r}_e;R)$ at some suitably large value of r_e [76]. To obtain moments for comparison to experimentally measured values we must vibrationally average these functions of R over the proba-

bility density of the ground vibrational state. Doing so yields $\langle\phi_0|\alpha_0|\phi_0\rangle = 5.376a_0^3$ and $\langle\phi_0|\alpha_2|\phi_0\rangle = 1.410a_0^3$, in good agreement with the experimental values of $5.4265a_0^3$ and $1.3567a_0^3$, respectively [77,78]. This agreement gives us confidence that, at least in the "extra-core" region, $V^A(\mathbf{r}_e;R)$ accurately represents induced polarization effects.

There is, of course, an important region outside the core where the adiabatic potential has *not* reduced to its asymptotic form (10). In this intermediate-r region, correlation and velocity-dependent (nonadiabatic) effects are negligible, because the target charge density is rapidly decaying to zero and the region of strong electron-nuclear attraction is too far away to affect the projectile's local kinetic energy; but here the polarization potential depends on r in a more complicated way than given by Eq. (10) [73].

The step from this adiabatic potential to the BTAD model is short but approximate. Following an idea first proffered by Temkin in a polarized-orbital study of electron-atom scattering [29], we correct $V^A(\mathbf{r}_e;R)$ in the core region by "turning off" the two-particle bound-free Coulomb interactions whenever the coordinate of the projectile is less than that of one of the bound electrons. In practice, this "nonpenetrating" approximation amounts to modifying the matrix elements of $V_{\rm em}$ [see Eq. (9)] by replacing the usual multipole expansion of the electron-electron Coulomb potential as follows:

$$\frac{1}{|\mathbf{r}-\mathbf{r}_e|} \rightarrow \begin{cases} \dfrac{r}{r_e^2}\cos\theta_e\ , & r_e \geq r\ , \\ 0\ , & r_e \leq r\ , \end{cases} \tag{11}$$

where we note that we have also retained only the dipole term in the multipole expansion. In our original study of the BTAD e-H_2 potential [31] we demonstrated that *for this system*, higher-order terms in this expansion result in changes to the cross section of less than 1% (the limit of numerical accuracy of these calculations) and that neglect of the monopole term is consistent with our theoretical formulation of the polarization phenomenon [30]. However *ad hoc*, the nonpenetrating approximation does properly weaken the polarization potential in the near-target region [7], and for electron-atom systems, models nonadiabatic effects with the correct dependence on r_e [79]. In these respects it mimics the true nonlocal short-range effects.

III. RESULTS AND ANALYSIS

A. Interaction potentials

Since H_2 is only weakly aspherical, one can discern the most important features of the e-H_2 interaction potential by examining the two lowest-order Legendre projections in the expansion (3). Figure 2 shows the $\lambda=0$ and $\lambda=2$ projections of the static-exchange (SE) potential, in which correlation and polarization effects are completely neglected, and of several static-exchange-polarization (SEP) models. In order to show the relative strength of various components of the interaction in this figure, we have approximated the exchange potential using a local approximation, the free-electron-gas exchange potential, which has been optimized for study of vibrational and rotational excitation [80]. This model potential was *not* used in any of the scattering calculations reported in this paper.

Also shown is the asymptotic polarization potential equation (10) to which all the SEP potentials reduce as $r_e \rightarrow \infty$. Figure 3 shows the $0\rightarrow 1$ vibrational cross sections obtained when these potentials are used in scattering calculations as described in Sec. II A.

By far the most strongly attractive of the SEP potentials is that obtained by adding to the SE potential the *adiabatic* polarization potential equation (8), which entails no correction in the core region. Because it completely neglects nonadiabatic and correlation effects, this potential is unrealistically strong; it offers an extreme "upper limit" analogous to the "lower limit" of the SE potential.

More realistic are the two other SEP potentials in Fig. 2. In the SEP (BTAD) model, as discussed in Sec. II, the

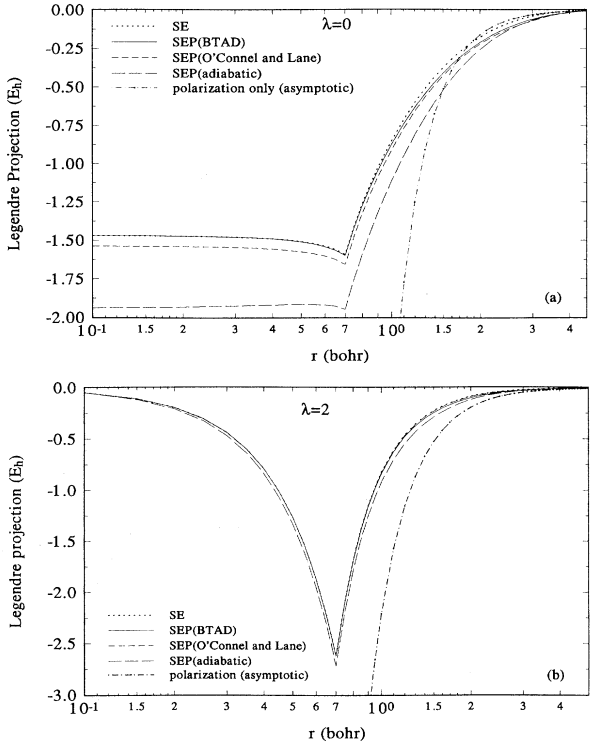

FIG. 2. (a) Spherical and (b) nonspherical Legendre projections of various model electron-H_2 interaction potentials in atomic units (hartrees) [see Eq. (3)]. The static-exchange potential (dotted curve) includes neither long-range polarization nor short-range (core-polarization) effects. The long-range *asymptotic* polarization potential (dash-dotted curve) is given by Eq. (10) and does not include static or exchange terms. The SEP adiabatic potential (long-dashed curve) includes all adiabatic polarization effects [see Eq. (8)] but no corrections in the core region. Finally, the BTAD (solid curve) and O'Connell and Lane (medium dashed curve) models are defined in the text. The internuclear separation is fixed at $1.402a_0$.

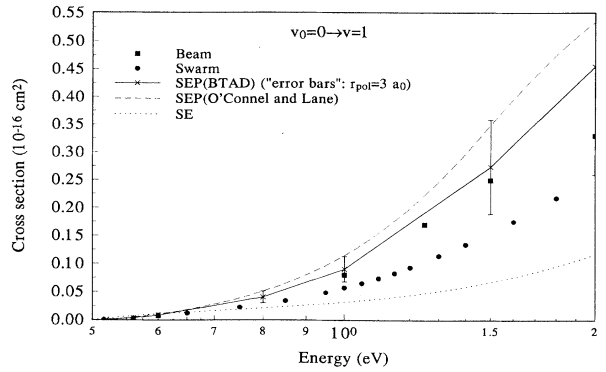

FIG. 3. Integral cross section for the $0\rightarrow 1$ excitation of H_2 as measured in crossed beam experiments of Brunger, Buckman, and Newman (Ref. [44]) (boxes) as derived by transport theory from swarm data by England, Elford, and Crompton (Ref. [46]) (closed circles) and as calculated by the present theory. In the latter, three treatments of polarization are shown: SE, i.e., complete omission of correlation and polarization effects (dotted curve), the BTAD model (solid curve with crosses), and the model of O'Connell and Lane (Ref. [81]) (dashed line). The "error bars" on the SEP (BTAD) theoretical results are based on the sensitivity analysis described in Sec. III.

nonpenetrating approximation properly weakens the polarization potential in the core region. The result, however, is still stronger than the SE potential—noticeably so beyond the cusp at $r_e=0.7a_0$.

The other SEP potential used in the present study was originally introduced defined by O'Connell and Lane for electron scattering from rare-gas atoms [81] and later adapted by Padial and Norcross to *vibrationally elastic* electron-molecule scattering, [82] where it has subsequently been widely applied [83]. The potential of O'Connell and Lane incorporates correlation of the projectile and the bound electrons of the frozen (i.e., unpolarized) target via an extremely simple analytic model based on the free-electron-gas correlation energy of density-functional theory, which one can calculate from the probability density of the ground electronic state of the target [84]. This model potential further incorporates long-range polarization effects (due to induced distortions of the target charge density) by the simple expedient of continuously joining the $\lambda=0$ and 2 projections of the short-range correlation potential to the asymptotic form (10) at the values of r_e where the two happen to intersect.

This second model potential has proven a useful approximation in some electron-molecule studies in the rigid-rotor approximation. But in a previous investigation of this potential for vibrational excitation of H_2 we found it to be too strong [24], producing cross sections which, as illustrated in Fig. 3, exceed both experimental results and those from BTAD calculations. In the present context, however, the model of O'Connell and Lane is extremely useful because it delimits (more realistically than the purely adiabatic potential) the magnitude of correlation-polarization effects for the cross sections of interest. This and the SE potential, then, evidently "bracket" the true polarization potential for vibrational excitation; and, as illustrated in Fig. 3, the corresponding cross sections can be considered upper and lower bounds on the correct values. If, for the sake of argument, one were to assume that the swarm-derived vibrational cross section is correct, then one would conclude from this figure that the BTAD is *too strong* in the core region, that the "true" short-range core-polarization potential should be weaker.

B. Assessing the sensitivity of cross sections to core polarization

Whenever one seeks to use comparisons to experimental data either to assess model potentials or to determine which approximations in a scattering calculation may require more rigorous treatment, one inevitably faces a key interpretive question: For which scattering quantities and in which energy ranges does one see the greatest sensitivity to various kinds of interactions? In the e-H_2 problem, for example, we are faced with excellent agreement between theory and several kinds of measured cross sections—integrated and differential total, momentum transfer, and rotational excitation—and a serious disagreement for vibrational excitation. In such a circumstance, what can one conclude about the accuracy of a model potential such as the BTAD?

This issue is complicated by the fact that while all these cross sections come from the same scattering matrix, some sample the potential differently than others. For example, as Fig. 4 illustrates, vibrationally elastic and inelastic cross sections are dominated by different blocks of this matrix: particularly at low energies the elastic cross section $\sigma^{(v)}_{0\rightarrow 0}$ (which for e-H_2 is by far the largest contributor to the grand total cross section as measured in, say, time-of-flight experiments) is due to Σ_g elements of the *BFVCC* scattering matrix, while $\sigma^{(v)}_{0\rightarrow 1}$ (except very near threshold) is almost entirely due to Σ_u elements [85]. The Σ_g block ($\Lambda=0$ and even order partial waves $l=0,2,\ldots$) is most strongly influenced by the spherical projection of the potential, the $\lambda=0$ term in Eq. (3), and the element of the scattering matrix that contributes most to the elastic cross section ($l=l_0=0$, i.e., $s\rightarrow s$) feels the full effect of the SEP potential. By contrast, the most important elements of the Σ_u block for the inelastic cross section ($l=l_0=1$, i.e., $p\rightarrow p$, and $l=3$, $l_0=1$, i.e., $p\rightarrow f$) experience both $v_0(r_e,R)$ and $v_2(r_e,R)$ but are barred to an extent from the short-range region by the centrifugal barrier [$l>0$ in Eqs. (1)].

Further complicating the picture is the sensitivity of some cross sections to properties of the scattering matrix that little affect others. For example, vibrational excitation cross sections are influenced far more by the R variation of the interaction potential than are elastic or rotational excitation cross sections. In fact, at energies far enough above threshold that the adiabatic-nuclear vibration approximation is valid [20], one can estimate the vibrational cross section from the first derivative with R of the Σ_u eigenphase sum [2].

We have therefore developed a strategy which will allow us to use these features of low-energy electron-molecule scattering to gain insight into short-range corre-

lation effects (in the e-H_2 system) by examining the sensitivities of various cross sections *to the near-target part* of the correlation-polarization potential, the only part that the BTAD model treats approximately. To this end we have performed a series of scattering calculations in which we remove this potential for all values of r_e outside a radius $r_{\rm pol}$, which we can vary from $r_{\rm pol}=0$ (the "no-polarization" or SE limit) to $r_{\rm pol}\to\infty$ (the "full-polarization" or SEP limit).

This strategy is summarized in Fig. 5. For $r_e > r_{\rm pol}$, we simply set the BTAD potential to zero but retain the full static and exchange interactions, including the long-range permanent quadrupole term $-[q(R)/r_e^3]P_2(\cos\theta_e)$ of the former. For each $r_{\rm pol}$ we solve the BFVCC scattering equations (1) on a discrete mesh of radial values from $r_e=0$ to $r_e=r_{\rm max}=180a_0$, where we extract the K matrix of Eq. (6) and calculate cross sections as functions of energy and, parametrically, of $r_{\rm pol}$. By comparing these cross sections to the limiting SE and SEP values we can determine, somewhat indirectly, the relative importance of the core-polarization interaction for $r < r_{\rm pol}$.

C. Total and momentum-transfer cross sections

Of all low-energy electron-molecule cross sections, those presently most amenable to accurate experimental determination are the total cross sections $\sigma_{\rm tot}$—technically, this is the grand total cross section, i.e., the sum of elastic, rotational, and vibrational cross sections which is measured in time-of-flight experiments such as those of Ferch, Raith, and Schroder [86] and Jones [71]—and the momentum-transfer cross section $\sigma_{\rm mom}$. The latter, at energies below the first inelastic threshold, can be determined uniquely and to high precision via the analysis of properties of a swarm of electrons drifting and diffusing through a gas of H_2 molecules (of number density N) under the influence of an applied electric field of strength $\mathcal{E}$ [87]. It is therefore to comparisons with $\sigma_{\rm tot}$ and $\sigma_{\rm mom}$ (also the most straightforward to calculate from theory) that one would likely turn to assess approximations in a scattering theory or potential. So it is here we begin our examination of sensitivity to the short-range part of the BTAD model correlation-polarization potential.

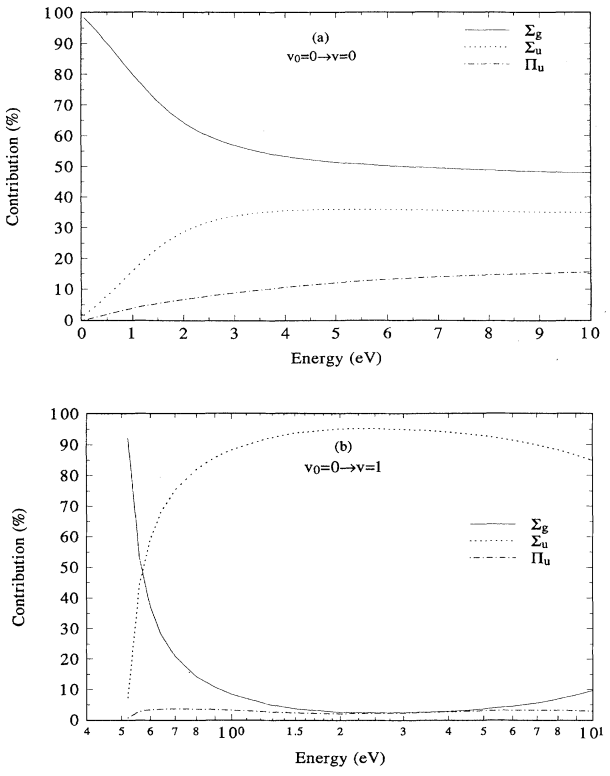

FIG. 4. Contributions to the e-H_2 (a) vibrationally elastic and (b) vibrationally inelastic ($0\to1$) cross section from the four dominant symmetries of the BFVCC scattering matrix: Σ_g (solid curve), Σ_u (dotted curve), and Π_u (dot-dashed curve). These percentages are based on SEP (BTAD) theoretical cross sections.

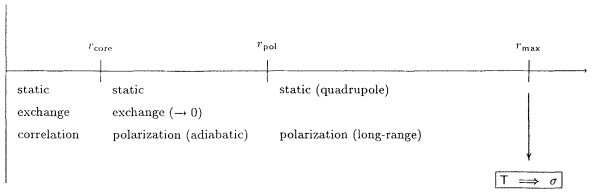

FIG. 5. Electron-molecule interactions and the regions of space in which they dominate. The radius of the core is $r_{\rm core}$, which for H_2 we take to be $\approx 2.5a_0$. By a radius of $r_{\rm max}$ the scattering wave function has settled down to its asymptotic form and one can extract the T matrix. Finally, $r_{\rm pol}$ is the floating polarization-elimination radius: in the present sensitivity analyses, the polarization interaction is "switched off" for $r_e > r_{\rm pol}$ and the result compared to SE ($r_{\rm pol}=0$) and full SEP ($r_{\rm pol}=r_{\rm max}\approx\infty$) calculations to determine the contribution of core polarization to the cross section in question [see Eq. (12)].

In Fig. 6 we see that both the integral total and momentum-transfer cross sections evince excellent agreement between theory and experiment and, especially at low energies, a pronounced sensitivity to correlation-polarization effects as manifested by the striking differences between SE and SEP (BTAD) values. At $E=0.047$ eV, for example, $\sigma_{\rm mom}$ in Fig. 6(b) decreases by 46% from the SE value (16.82 Å^2) to the SEP limit (8.78 Å^2), which agrees well with the swarm-derived value (9.05 Å^2). The grand total cross sections of Fig. 6(a) exhibits similar behavior. At $E=0.3$ eV, for instance, $\sigma_{\rm tot}$ drops by 32% from its SE value (15.71 Å^2) to its SEP (BTAD) value (10.59 Å^2), which agrees splendidly with that obtained by Ferch, Raith, and Schroder in time-of-flight measurements (10.71 Å^2) [86].

Such graphs, however, somewhat misrepresent the influence of correlation and polarization effects because the eigenphase shift corresponding to the dominant element of the dominant block of the scattering matrix for these cross sections—the $l=l_0=0$; $v=v_0=0$ element of the Σ_g T-matrix —passes through a multiple of $3\pi/4$ as the energy decreases and approaches π at zero energy. This influence is more clearly represented by the Σ_g

eigenphase sum $\delta_{\text{sum}}^{\Sigma_g}$ as shown in Fig. 7. Here we see that inclusion of the correlation-polarization potential (by increasing r_{pol} from 0 to ∞) strengthens the total interaction potential and increases $\delta_{\text{sum}}^{\Sigma_g}$ accordingly.

We also see that the greatest changes in this eigenphase sum (and σ_{tot} and σ_{mom}) arise from correlation-polarization effects *outside the core*. This behavior is especially striking at low energies. Thus at $E=0.047$ eV, the momentum-transfer cross section for $r_{\text{pol}}=4$ (15.49 Å^2), a radius clearly outside the core, is quite close to its SE value; at such energies, then, the decrease of σ_{mom} to the SEP limit occurs in the asymptotic (large r_e) region. Returning to the graphs of cross sections in Fig. 6 we note that σ_{tot}, say, is not particularly sensitive to *core polarization*; at 0.3 eV, for example, its value for $r_{\text{pol}}=3.0a_0$ (15.19 Å^2) differs from the SE limit by only 3%.

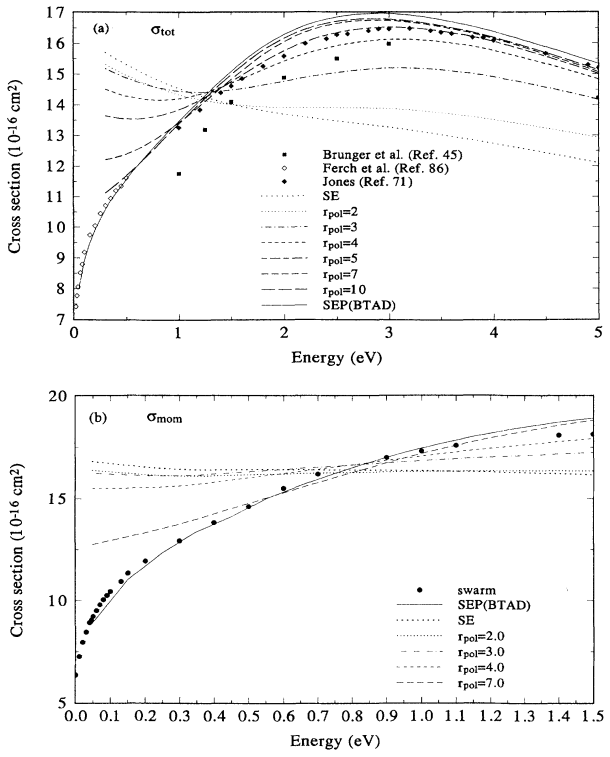

FIG. 6. (a) The grand total and (b) momentum-transfer cross sections for e-H_2 scattering. In (a), the experimental data are from crossed-beam experiment by Brunger, Buckman, and Newman (Ref. [44]) (boxes), time-of-flight measurements by Ferch, Raith, and Schroder (Ref. [86]) (open diamonds), and by Jones (Ref. [71]) (closed diamonds). In (b), the experimental cross sections (closed circles) are derived from swarm data of England, Elford, and Crompton (Ref. [87]). In both figures, the theoretical results come from scattering calculations in which correlation and polarization effects are excluded entirely (the SE limit) (dotted curve), in which they are included via the BTAD potential (solid curve), and in which they are partially included by varying r_{pol} in sensitivity analysis like those in Fig. 8. Several such analyses are shown: $r_{\text{pol}}=2.0a_0$ (tiny-dashed curve), $r_{\text{pol}}=3.0a_0$ (dot-dashed curve), $r_{\text{pol}}=4.0a_0$ (short-dashed curve), $r_{\text{pol}}=5.0a_0$ (long-dash–short-dashed curve), $r_{\text{pol}}=7.0a_0$ (medium-dashed curve), and $r_{\text{pol}}=10.0a_0$ (long-dashed curve).

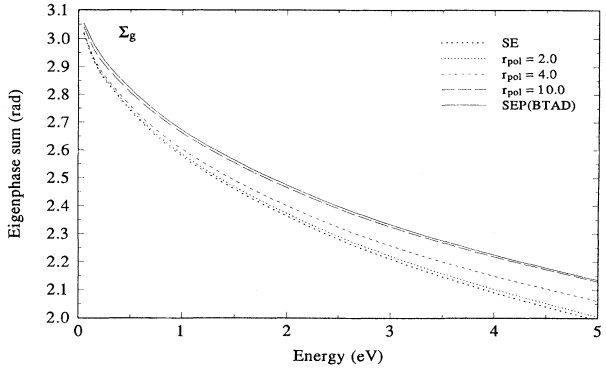

FIG. 7. Eigenphase sums in the Σ_g electron-molecule symmetry for vibrationally elastic e-H_2 scattering from static-exchange (dotted curve) and SEP (BTAD) (solid curve) calculations. Also shown are results for cutoff radii r_{pol} (in a_0) for core polarization of 2.0 (tiny-dashed curve) and 4.0 (long-dashed curve).

Energies below 1 eV are especially important, for it is here that transport analysis should be most accurate in determining the momentum-transfer and inelastic cross sections [35]. In regard to the excellent agreement between theoretical and swarm-derived values for σ_{mom} in Fig. 6(b), it is important to note that these cross sections emerge from the same transport analysis that yields the more contentious vibrational cross sections seen in Fig. 1. The point is that just as a certain consistency inheres in all theoretical scattering quantities derived from the same scattering matrix (and, of course, the same interaction potential), so do all swarm-derived cross sections—momentum-transfer, rotational excitation, and vibrational excitation—correspond to a single set of single set of transport data. Although different ranges of $\mathcal{E}/N$ (the ratio of the strength of the applied electric field to the number density of target molecules) govern these various cross sections, together they comprise the cross-section set used to calculate the electron energy distribution function via solution of the Boltzmann equation. This function, in turn, is used to calculate transport properties such as the drift velocity (the velocity with which electrons in the swarm drift through the target gas under the influence of the applied field) for comparison to measured properties [34,37].

At 1.0 eV, most of the 6% difference between the SE (16.36 Å^2) and SEP(BTAD) (17.36 Å^2) momentum-transfer cross sections is due to polarization from $r_e \geq 3a_0$. Above 1.0 eV, both correlation and polarization effects are less important to σ_{tot} and σ_{mom} than the static and exchange interactions. So studies of these cross sections are not particularly fallow fields for investigation of these effects. But even at lower energies, where polarization is more important, the comparative insensitivity of σ_{tot} and σ_{mom} to *core-polarization* effects precludes our concluding anything definitive from this agreement about the accuracy of the short-range approximations in the BTAD potential. And so we now turn to inelastic cross sections.

D. Inelastic cross sections

Although direct comparisons of cross sections as a function of energy for various r_{pol} such as those in Fig. 6 are illuminating, they can become cumbersome if several excitations and energies are of interest; in some cases, they even obscure the essential physics that motivates the investigation in the first place. An alternative way to represent the effect of core polarization is to look at the desired cross section *as a function of* r_{pol} *for fixed energy*; this approach admits introduction of a single quantity which characterizes the effects we wish to study.

For example, let us consider the $0\rightarrow 1$ vibrational excitation at $E=1.0$ eV. Not only is this an energy where the disagreements over the value of this cross section are quite great—the difference between the theoretical and swarm-derived values for $\sigma_{0\rightarrow 1}^{(v)}$ at this energy is 59%—it is also one where, as we see in Fig. 8 polarization is very important. The SE cross section $\sigma_{0\rightarrow 1}^{(v)}$ at this energy (0.0317 Å^2), indicated by the lower horizontal line in this figure, lies 65% below the SEP (BTAD) value (0.0948 Å^2), the upper horizontal line. The solid circles show the effect of selectivity eliminating correlation and polarization interactions by varying r_{pol} between these limits. This figure, therefore, exhibits the change in $\sigma_{0\rightarrow 1}^{(v)}$ as r_{pol} is varied between the SE and SEP (BTAD) limits. For example, the value for $r_{pol}=2.0a_0$ is 0.0353 Å^2; that for $r_{pol}=3.0a_0$ is 0.0468 Å^2. We see that at this energy polarization *outside the core* most affects this cross section: very little of the 65% difference between the SE and SEP (BTAD) values is due to polarization for $r<r_{pol}=2.0a_0$.

As this analysis illustrates, the salient quantity in assessing the importance of core polarization is the *relative* difference between a result for a particular r_{pol} and the SE and SEP limits. We can conveniently collapse this information into a single number by defining *the relative percentage difference* of the SEP (BTAD) cross section from its counterpart for finite r_{pol}, which we denote by $\sigma(r_{pol})$:

$$P_{pol}(r_{pol})\equiv\left[1-\frac{\sigma(\mathrm{SEP})-\sigma(r_{pol})}{\sigma(\mathrm{SEP})-\sigma(\mathrm{SE})}\right]\times 100\ . \qquad (12)$$

The crosses in Fig. 8 (right-hand scale) show this quantity as a function of r_{pol} for $\sigma_{0\rightarrow 1}^{(v)}$ at 1.0 eV. Thus Eq. (12) gives 6% for the fraction of the SEP (BTAD) cross section attributable to polarization within $2.0a_0$, and 25% for $r_{pol}=3.0a_0$.

Since the static, exchange, and polarization components of the interaction are not strictly additive in their effect on various cross sections, this quantity offers only a rough indication of sensitivity to core polarization, within our theoretical model. Still, for all scattering processes discussed in this paper we have found that P_{pol} accurately reflects the "accumulation" of core polarization exemplified by more capacious representations such as Fig. 8. These percentages, in turn, are shown in Fig. 9 *as a function of energy* (for two values of r_{pol} near the core) for both rotational and vibrational excitation.

The first thing one notices about the percentages in Fig. 9 is that the sensitivity of $\sigma_{0\rightarrow 2}^{(r)}$ and $\sigma_{0\rightarrow 1}^{(v)}$ to core polarization increases with energy. Near threshold, where transport analysis of swarm data should be most accurate and crossed-beam measurements are infeasible, these cross sections are not highly sensitive to core polarization. At $E=0.6$ eV, for example, the SE vibrational cross section (0.0104 Å^2) exceeds the SEP value (0.0077 Å^2) by 26%. By varying r_{pol}, however, we find that $\sigma_{0\rightarrow 1}^{(v)}$ at this energy changes very little between the SE limit ($r_{pol}=0$) and values for r_{pol} well outside the core. Even for $r_{pol}=7.0a_0$, well into the asymptotic region, it has decreased from its SE value by only 5% (to 0.0099 Å^2). Thus near-threshold vibrational excitation is primarily determined by the static and exchange interactions; polarization influences this quantity but primarily in the asymptotic region. So near-threshold vibrational cross sections are of limited value as indicators of the accuracy of models of core polarization.

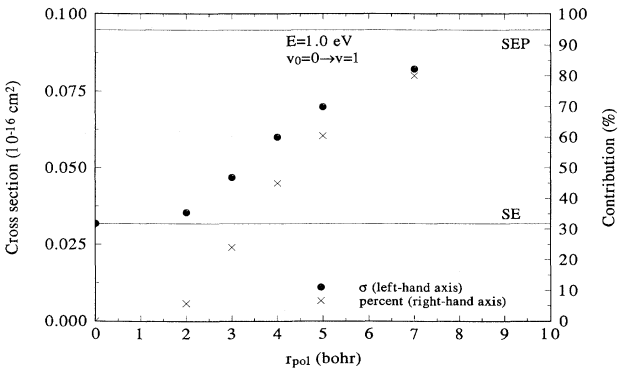

FIG. 8. A sensitivity analysis of the $0\rightarrow 1$ vibrational cross section of H_2 at $E=1.0$ eV (see Fig. 3). This cross section (closed circles and left-hand axis) and the percent contribution to it due to core polarization [see Eq. (12)] (crosses and right-hand axis) are shown as functions of the radius r_{pol} beyond which polarization effects are eliminated (see Sec. III B). The horizontal lines are the SE (lower) and SEP(BTAD) (upper) cross sections, where the latter corresponds to the limit $r_{pol}\rightarrow\infty$.

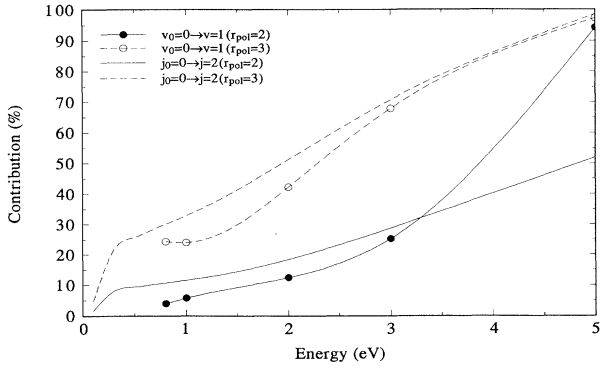

FIG. 9. The percent contribution of core polarization to the $v_0=0\rightarrow v=1$ vibrational cross section (curves with symbols) and the $j_0=0\rightarrow j=2$ rotational cross section (curves without symbols). This quantity, defined in Eq. (12), is shown for two near-core values of the polarization elimination radius r_{pol}: $2.0a_0$ (solid lines) and $3.0a_0$ (dotted lines).

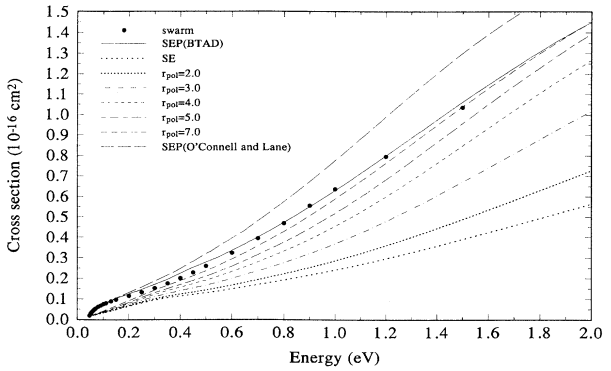

FIG. 10. Cross sections for the $j_0=0\rightarrow j=2$ rotational excitation from transport analysis of swarm data by England, Elford, and Crompton (Ref. [87]) (closed circles) and various theoretical calculations. The SE limit (dotted curve) excludes correlation and polarization effects, while the SEP cross sections were calculated using the BTAD potential (solid curve) and using the model of O'Connell and Lane (Ref. [81]) (long-dashed curve) as discussed in Secs. II and III A. In addition, theoretical results from the following limited-range polarization studies are shown: $r_{\rm pol}=2.0a_0$ (tiny-dashed curve), $r_{\rm pol}=3.0a_0$ (dot-dashed curve), $r_{\rm pol}=4.0a_0$ (short-dashed curve), $r_{\rm pol}=5.0a_0$ (long-dash–short-dashed curve), $r_{\rm pol}=7.0a_0$ (medium-dashed curve).

As the energy increases from threshold (at 0.52 eV), however, the sensitivity of $\sigma^{(v)}_{0\rightarrow 1}$ to core polarization rapidly increases. Because of continuing concern about the discrepancy between theory and various experiments at energies below 2.0 eV [8,27] we have used the percent differences for $r_{\rm pol}=3.0a_0$ to generate crude "error bars" on the theoretical SEP (BTAD) cross sections in Fig. 3. These estimates are probably too pessimistic; still, they do provide a visualization of the sensitivity of our theoretical cross section to core polarization. In particular, they suggest that it is unlikely that reasonable changes in the near-target correlation potential would bring the theoretical vibrational cross sections into alignment with swarm-derived values.

We shall conclude with a look at the $0\rightarrow 2$ rotational excitation cross section in Fig. 10. This cross section is of interest in conjunction with $\sigma^{(v)}_{0\rightarrow 1}$ for three reasons. First, like the vibrational cross section, it is dominated by the Σ_u symmetry (except very near threshold). Second, as the percentages in Fig. 9 show, its sensitivity to core polarization is comparable to that of $\sigma^{(v)}_{0\rightarrow 1}$, increasing rapidly with energy in both cases. Finally, *unlike* the vibrational cross section, rotational cross sections from our SEP (BTAD) calculations and transport analysis of swarm data agree very well [87,88].

IV. CONCLUSIONS AND OUTLOOK

Within a frame defined by BFVCC theory of electron-molecule scattering, using static and (exact) exchange potentials based on a near-Hartree-Fock wave function and polarization outside the core determined by a linear variational calculation which reproduces the correct asymptotic dependence on the molecular polarizability tensor, we have explored the influence of core polarization on a variety of cross sections. Our goal was to identify scattering processes and energy ranges which are particularly sensitive to this effect, partly as a guide to assessments of models such as the nonpenetrating approximation incorporated in the present BTAD potential. Additionally, we have sought to provide insight into whether a more rigorous (and much more arduous) treatment of short-range bound-free correlation and nonadiabatic effects would likely remove the severe discrepancy between theoretical, swarm-derived, and beam-measured cross sections for the $0\rightarrow 1$ vibrational excitation of H_2.

Although we have therefore emphasized the e-H_2 system, some of our qualitative findings should have validity beyond this immediate context. The comparative insensitivity to core polarization of total and momentum-transfer cross sections illustrated in Fig. 6 is probably not unique to this system, since it is due in large part to the dominance of elastic scattering. Similarly, the rapid increase in the sensitivity of rotational and vibrational cross sections above threshold evident in Fig. 9 should generalize to nonresonant collisions for other systems.

The findings of the present study in no way diminish the need for vibrational excitation calculations in which bound-free correlation is treated correctly as a many-body phenomenon. While the comparisons in Sec. III suggest that reasonable alterations to this potential in the core are unlikely to produce vibrational cross sections that conform to the measured transport data for H_2 without seriously compromising the rotational (and perhaps total and momentum transfer) cross sections, one can be no more definitive without access to results from vibrational excitation calculations that *rigorously* include many-body correlation effects. If such an enterprise is undertaken, the technical and computational difficulties of carrying out such calculations argue for abandoning full vibrational coupling in favor of an approximate treatment of the vibrational dynamics that is appropriate to these energies, such as the first-order nondegenerate adiabatic theory [89].

Until such results are available, the situation remains clouded with uncertainty. The analyses of the present study support the results of the recent crossed-beam experiments of Brunger *et al.* [45] but are at odds with a recent error analysis by Crompton and Morrison [35] of the swarm experiments. Given that such experiments remain the only proven source of very-low-energy integrated cross sections for wide variety of systems, the inability of theory and experiment to agree on this simple excitation process in this simplest of neutral molecules is most disturbing.

ACKNOWLEDGMENTS

We would like to thank Dr. Neal Lane, Dr. Aaron Temkin, Dr. Thomas L. Gibson, Dr. Robert W. Crompton, Dr. Thomas Rescigno, Dr. Stephen J. Buckmann, and Dr. David Norcross for invaluable conversations concerning various aspects of this research. We are particularly grateful to Dr. Barbara Whitten for several ex-

cellent suggestions based on a thoughtful reading of an earlier version of this manuscript. One of us (M.A.M.) would also like to thank the Joint Institute for Laboratory Astrophysics, which he was visiting during the period that most of this work was completed, and to gratefully acknowledge the support by National Science Foundation Grant. No. PHY 9108890 and a grant of time on the CRAY 2 and XMP systems at the National Center for Supercomputing Applications at the University of Illinois at Urbana-Champaign. The other author (W.K.T.) would like to acknowledge partial support by NSF Grant No. PHY 9012244.

---

*Permanent address: Department of Physics & Astronomy, University of Oklahoma, Norman, OK 73019-0225. JILA Visting Fellow 1991-92.

[1] M. A. Morrison, Aust. J. Phys. **36**, 239 (1983).
[2] N. F. Lane, Rev. Mod. Phys. **52**, 29 (1980).
[3] M. A. Morrison, Adv. At. Mol. Phys. **24**, 51 (1988).
[4] A. D. Buckingham, Adv. Chem. Phys. **12**, 107 (1967).
[5] L. Castillejo, I. C. Percival, and M. J. Seaton, Proc. R. Soc. London, Ser. A. **254**, 259 (1960).
[6] M. J. Seaton and L. Steenman-Clark, J. Phys. B **10**, 2639 (1977); **11**, 293 (1978).
[7] C. J. Kleinman, Y. Hahn, and L. Spruch, Phys. Rev. A **165**, 53 (1968).
[8] For a summary see R. W. Crompton and M. A. Morrison, in *Swarm Studies and Inelastic Electron-Molecule Scattering,* edited by L. C. Pitchford, V. McKoy, A. Chutjian, and S. Trajmar (Springer-Verlag, Berlin, 1986).
[9] Important earlier work on polarization in electron-molecule scattering includes B. I. Schneider, Chem. Phys. Lett. **51**, 578 (1977); and A. Klonover and U. Kaldor, J. Phys. B **12**, L61 (1979).
[10] D. G. Truhlar, D. A. Dixon, and R. A. Eades, J. Phys. B **12**, 1913 (1979); D. A. Dixon, R. E. Eades, and D. G. Truhlar, *ibid.* 2471 (1979); R. A. Eades, D. G. Truhlar, and D. A. Dixon, Phys. Rev. A **20**, 867 (1979); R. A. Eades, D. A. Dixon, and D. G. Truhlar, J. Phys. B **15**, 2265 (1982).
[11] See, for example, B. I. Schneider, Chem. Phys. Lett. **51**, 578 (1977); R. K. Nesbet, C. J. Noble, L. A. Morgan, and C. A. Weatherford, J. Phys. B **17**, L891 (1984); M. Le Dorneuf, V. Lan, and P. G Burke, Comments At. Mol. Phys. **7**, 1926 (1977). For applications to atoms, see P. G. Burke, C. J. Noble, and S. Salvini, J. Phys. B **16**, L113 (1983).
[12] J. R. Taylor, *Scattering Theory* (Wiley, New York, 1972).
[13] R. G. Newton, *Scattering Theory of Waves and Particles,* 2nd ed. (Springer-Verlag, New York, 1982).
[14] H. D. Meyer, Phys. Rev. A **40**, 5605 (1989).
[15] B. I. Schneider and L. A. Collins, J. Phys. B **15**, L335 (1982); Phys. Rev. A **27**, 2847 (1983).
[16] H. D. Meyer, J. Phys. B **25**, 2657 (1992).
[17] C. J. Gillan, O. Nagy, P. G. Burke, L. A. Morgan, and C. J. Noble, J. Phys. B **20**, 4585 (1987).
[18] K. Takatsuka and V. McKoy, Phys. Rev. A **24**, 2473 (1981); K. Takatsuka and V. McKoy, *ibid.* **30**, 1734 (1984); T. L. Gibson, M. A. P. Lima, K. Takatsuka, and V. McKoy, *ibid.* **30**, 3005 (1984); M. Berman and U. Kaldor, J. Phys. B **14**, 3993 (1981); Chem. Phys. Lett. **79**, 489 (1981).
[19] T. N. Rescigno, C. W. McCurdy, and B. I. Schneider, Phys. Rev. Lett. **63**, 248 (1989); T. N. Rescigno, B. H. Lengsfield III, and C. W. McCurdy, Phys. Rev. A **41**, 2462 (1990); A. E. Orel, T. N. Rescigno, and B. H. Lengsfield III, *ibid.* **42**, 5292 (1990); S. D. Parker, C. W. McCurdy, T. N. Rescigno, and B. H. Lengsfield III, *ibid.* **43**, 3514 (1991); B. I. Schneider, T. N. Rescigno, B. H. Lengsfield III, and C. W. McCurdy, Phys. Rev. Lett. **66**, 2728 (1991); B. H. Lengsfield III, T. N. Rescigno, and C. W. McCurdy, Phys. Rev. A **44**, 4296 (1991); W. Sun, C. W. McCurdy, and B. H. Lengsfield III, *ibid.* **45**, 6323 (1992).
[20] A. Temkin and F. H. M. Faisal, Phys. Rev. A **3**, 520 (1971); S. Hara, J. Phys. Soc. Jpn. **27**, 1592 (1969); E. S. Chang and A. Temkin, Phys. Rev. Lett. **23**, 389 (1969).
[21] For an alternative to the rigid rotor approximation which improves the accuracy of cross section without requiring coupling of vibrational motion, see W. K. Trail, M. A. Morrison, W. A. Isaacs, and B. C. Saha, Phys. Rev. A **41**, 4868 (1990).
[22] R. J. W. Henry, Phys. Rev. A **2**, 1349 (1970).
[23] M. A. Morrison, B. C. Saha, and A. N. Feldt, Phys. Rev. A **30**, 2811 (1984).
[24] M. A. Morrison and B. C. Saha, Phys. Rev. A **34**, 2786 (1986).
[25] J. R. Rumble, D. G. Truhlar, and M. A. Morrison, J. Chem. Phys. **79**, 1846 (1983).
[26] M. A. Morrison, A. N. Feldt, and D. A. Austin, Phys. Rev. A **29**, 2518 (1984).
[27] Stephen J. Buckman, M. J. Brunger, D. S. Newman, G. Snitchler, S. Alston, D. W. Norcross, Michael A. Morrison, B. C. Saha, G. Danby, and W. K. Trail, Phys. Rev. Lett. **65**, 3253 (1990).
[28] M. A. Morrison, B. C. Saha, and T. L. Gibson, Phys. Rev. A **36**, 3682 (1987).
[29] A. Temkin, Phys. Rev. **107**, 1004 (1957).
[30] T. L. Gibson, Ph. D. thesis, University of Oklahoma, 1982.
[31] T. L. Gibson and M. A. Morrison, Phys. Rev. A **29**, 2497 (1984); J. Phys. B **15**, L221 (1982).
[32] N. F. Lane and R. J. W. Henry, Phys. Rev. A **173**, 183 (1968).
[33] A. Temkin and J. C. Lamkin, Phys. Rev. **121**, 788 (1961).
[34] M. A. Morrison, R. W. Crompton, B. C. Saha, and Z. Lj. Petrović, Aust. J. Phys. **40**, 239 (1987).
[35] R. W. Crompton and M. A. Morrison, Aust. J. Phys. **46**, 203 (1993).
[36] The "Bible" of transport theory is L. G. H. Huxley, R. W. Crompton, *The Diffusion and Drift of Electrons in Gases* (Wiley, New York, 1974).
[37] Useful introductions to the theory can be found in the review by L. G. H. Huxley and R. W. Crompton, in *Atomic*

and Molecular Processes, edited by D. R. Bates, (Academic, New York, 1962), Chap. 10; and in R. W. Crompton, Adv. Electron. Electron Phys. **27**, 1 (1969). On the importance of swarm-derived cross sections, see R. W. Crompton, Aust. Physicist **25**, 146 (1988).

[38] R. W. Crompton, D. K. Gibson, and A. I. McIntosh, Aust. J. Phys. **22**, 715 (1969).

[39] R. W. Crompton, D. K. Gibson, and A. G. Robertson, Phys. Rev. A **2**, 1386 (1970).

[40] R. W. Crompton, M. T. Elford, and A. G. Robertson, Aust. J. Phys. **23**, 667 (1970).

[41] H. Ehrhardt, L. Langhans, F. Linder, and H. S. Taylor, Phys. Rev. **173**, 222 (1968).

[42] F. Linder and H. Schmidt, Z. Naturforsch. Teil A **26**, 1603 (1971).

[43] H. Nishimura, A. Danjo, and H. Sugahara, J. Phys. Soc. Jpn. **54**, 1757 (1985).

[44] M. J. Brunger, S. J. Buckman, and D. S. Newman, D. S., Aust. J. Phys. **43**, 665 (1990).

[45] M. J. Brunger, S. J. Buckman, D. S. Newman, and D. T. Alle, J. Phys. B **24**, 1435 (1991).

[46] J. P. England, M. T. Elford, and R. W. Crompton, Aust. J. Phys. **41**, 573 (1988).

[47] For a summary of recent advances in the application of transport theory, see R. W. Crompton, in *Proceedings of the Sixteenth International Conference on Phenomena in Ionized Gases, Invited Papers,* edited by C. Bötticher *et al.* (University of Düsseldorf, Düsseldorf, 1983), p. 58.

[48] A. Englehardt and A. V. Phelps, Phys. Rev. **131**, 2115 (1963).

[49] D. K. Gibson, Aust. J. Phys. **23**, 683 (1970).

[50] A. G. Engelhardt, A. V. Phelps, and C. G. Risk, Phys. Rev. **135**, A 1556 (1964); G. Haddad, Aust. J. Phys. **37**, 487 (1984); H. Tagashira, T. Tanaguchi, and T. Sakai, J. Phys. D **13**, 235 (1980); D. Levron and A. V. Phelps, Bull. Am. Phys. Soc. **24**, 129 (1979); K. Tachibana and A. V. Phelps, J. Chem. Phys. **71**, 3544 (1979).

[51] R. D. Hake and A. V. Phelps, Phys. Rev. **158**, 70 (1967).

[52] J. J. Lowke, A. V. Phelps, and B. W. Irwin, J. Appl. Phys. **14**, 615 (1976); B. R. Bulos and A. V. Phelps, Phys. Rev. A **14**, 615 (1976).

[53] G. E. Haddad and M. T. Elford, J. Phys. B **12**, L743 (1979).

[54] G. N. Haddad and H. B. Milloy, Aust. J. Phys. **36**, 473 (1983).

[55] R. E. Voshall and A. V. Phelps, Phys. Rev. **127**, 2084 (1962); K. F. Ness and R. E. Robson, Phys. Rev. A **38**, 1446 (1988).

[56] C. W. Duncan and I. C. Walker, Trans. Faraday Soc. II **68**, 1514 (1972); L. C. Pitchford, S. V. O'Neil, and J. R. Rumble, Phys. Rev. A **23**, 294 (1981); G. N. Haddad, Aust. J. Phys. **38**, 677 (1985).

[57] W. K. Trail, Ph.D. thesis, University of Oklahoma, 1992.

[58] D. M. Chase, Phys. Rev. A **104**, 838 (1956).

[59] E. S. Chang and U. Fano, Phys. Rev. A **6**, 173 (1972).

[60] M. Shugard and A. U. Hazi, Phys. Rev. A **12**, 1975 (1975).

[61] A. Temkin and K. V. Vasavada, Phys. Rev. A **160**, 190 (1967); A. Temkin, K. V. Vasavada, E. S. Chang, and A. Silver, *ibid.* **186**, 57 (1969); S. Hara, J. Phys. Soc. Jpn. **27**, 1592 (1969).

[62] N. Chandra and A. Temkin, Phys. Rev. A **13**, 188 (1976).

[63] A. M. Arthurs and A. Dalgarno, Proc. R. Soc. London, Ser. A **256**, 540 (1960); N. F. Lane and S. Geltman, Phys. Rev. **160**, 53 (1967); R. J. W. Henry and N. F. Lane, *ibid.* **183**, 221 (1969).

[64] M. A. Morrison, Comput. Phys. Commun. **21**, 63 (1980).

[65] L. A. Collins, D. W. Norcross, and G. B. Schmid, Comput. Phys. Commun. **79**, 63 (1980).

[66] Explicit forms for the exchange matrix elements can be found in Ref. [21]. See also Refs. [3,57].

[67] B. I. Schneider and L. A. Collins, J. Phys. B **14**, L101 (1981); L. A. Collins and B. I. Schneider, Phys. Rev. A **24**, 2387 (1981); **27**, 101 (1983); B. I. Schneider and L. A. Collins, J. Phys. B **33**, 2982 (1986).

[68] W. N. Sams and D. J. Kouri, J. Chem. Phys. **51**, 4809 (1969).

[69] M. A. Morrison, in *Electron- and Photon-Molecule Collisions,* edited by T. N. Rescigno, B. V. McKoy, and B. I. Schneider (Plenum, New York, 1979).

[70] L. A. Collins and B. I. Schneider, Comput. Phys. Rep. **10**, 49 (1989).

[71] R. K. Jones, Phys. Rev. A **31**, 2898 (1985).

[72] A. N. Feldt and M. A. Morrison, Phys. Rev. A **29**, 401 (1984).

[73] M. A. Morrison and P. J. Hay, Phys. Rev. A **20**, 740 (1979).

[74] See, for example, A. D. McLean and M. Yoshimine, J. Chem. Phys. **46**, 3682 (1967); M. A. Morrison and P. J. Hay, *ibid.* **79**, 4034 (1979).

[75] N. F. Lane and R. J. W. Henry, Phys. Rev. **173**, 183 (1968); S. Hara, J. Phys. Soc. Jpn. **27**, 1262 (1969).

[76] How large depends on the number of significant figures required. Hydrogen is so weakly polarizable that its adiabatic potential has settled down to Eq. (10) to two decimal places by $r_e \approx 4a_0$ and to three by $r_e \approx 7a_0$.

[77] K. B. MacAdam and N. F. Ramsey, Phys. Rev. A **6**, 898 (1972).

[78] A. C. Newell and R. C. Baird, J. Appl. Phys. **36**, 3751 (1965).

[79] J. Callaway, R. W. LaBahn, R. T. Pu, and W. M. Duxler, Phys. Rev. **168**, 12 (1968); Y. C. Jean and D. Schrader, Phys. Rev. A **18**, 2030 (1978); A. Dalgarno, G. W. F. Drake, and G. A. Victor, Phys. Rev. **176**, 194 (1968).

[80] M. A. Morrison and L. A. Collins, Phys. Rev. A **17**, 918 (1978), and references therein.

[81] J. K. O'Connell and N. F. Lane, Phys. Rev. A **27**, 1893 (1983).

[82] N. T. Padial and D. W. Norcross, Phys. Rev. A **29**, 1742 (1984).

[83] N. T. Padial and D. W. Norcross, Phys. Rev. A **29**, 1590 (1984); N. T. Padial, *ibid.* **32**, 1379 (1985); A. Jain and D. W. Norcross, *ibid.* **32**, 134 (1985); **34**, 739 (1986); P. K. Bhattacharyya, D. K. Syamal, and B. C. Saha, *ibid.* **32**, 854 (1985).

[84] J. P. Perdew and A. Zunger, Phys. Rev. A **29**, 1742 (1981).

[85] In the fixed nuclear orientation approximation, the projection Λ of the electronic orbital angular momentum along $\hat{\mathbf{R}}$ and the parity are good quantum numbers. Consequently the scattering matrix is diagonal with respect to these quantum numbers, and the integrated total and momentum-transfer cross sections can be expressed as sums of partial cross sections defined with respect to electron-molecule symmetries which are specified by these quantum numbers: Σ_g and Σ_u for $\Lambda=0$, Π_g and Π_u for $\Lambda=1$, and so forth. Eigenphase sums for these various symmetries are obtained by diagonalizing the relevant block of the K matrix, then summing the arctangents of the resulting elements.

[86] J. Ferch, W. Raith, and K. Schroder, J. Phys. B **13**, 1481 (1980).
[87] J. P. England, M. T. Elford, and R. W. Crompton, Aust. J. Phys. **41**, 573 (1988).
[88] R. W. Crompton, D. K. Gibson, and A. I. McIntosh, Aust. J. Phys. **22**, 715 (1969).
[89] M. A. Morrison, J. Phys. B **19**, L707 (1986); M. Abdolsalami and M. A. Morrison, Phys. Rev. A **36**, 5474 (1987); M. A. Morrison, M. Abdolsalami, and B. K. Elza, *ibid.* **43**, 3440 (1991).